

DOI 10.24425/ae.2023.146038

Comparative analysis of the power parameters of a line start permanent magnet synchronous motor using professional FEM packages and in-house software

MARIUSZ BARANSKI  

*Institute of Electrical Engineering and Electronics
Faculty of Control, Robotics and Electrical Engineering
Poznan University of Technology
Piotrowo 3A, 60-965 Poznan*

e-mail:  mariusz.baranski@put.poznan.pl

(Received: 02.03.2023, revised: 16.04.2023)

Abstract: The paper discusses the methods for calculating the power parameters of a line start permanent magnet synchronous motor (LSPMSM). The calculations have been performed using the author's specialized FEM software and professional FEM packages, ANSYS Maxwell and COMSOL Multiphysics. The author's algorithm for solving equations of the electromagnetic field based on the FEM has been presented. The in-house software developed on this algorithm and professional software have been used to analyse the power parameters of the LSPMS motor. In addition, both calculation time and accuracy were analysed. The calculation results were compared to the measurement results.

Key words: FEA, in-house software, measurement verification, professional FEM packages

1. Introduction

Rising energy prices are driving increased interest in high-energy electric machines. More than 40% of the world's electricity production is consumed by electric motors [1]. In industrial applications, induction machines (IMs) are still the first choice for electric drives. This is due to their simple design, high reliability, low operating costs and low price. IM motors have good start-up characteristics. On the other hand, the high reactive energy consumption, and additional losses in the rotor cage result in a relatively low efficiency and power factor compared, for example, to permanent magnet synchronous motors (PMSMs), which, compared to IMs, have a higher



© 2023. The Author(s). This is an open-access article distributed under the terms of the Creative Commons Attribution-NonCommercial-NoDerivatives License (CC BY-NC-ND 4.0, <https://creativecommons.org/licenses/by-nc-nd/4.0/>), which permits use, distribution, and reproduction in any medium, provided that the Article is properly cited, the use is non-commercial, and no modifications or adaptations are made.

power output for the same size. Unfortunately, the disadvantage of PMSMs is the need to use converter systems, which, among other things, increases the price of the drive. For constant-speed drives, this cost can be minimized by implementing line-start permanent magnet synchronous motors (LSPMSMs), which use permanent magnets to generate the magnetic field in a rotor with a start-up rotor cage [2, 3]. Such motors are widely applied in industry, e.g., as drives for pumps or fans [4, 5].

LSPMSMs have many advantages, such as a high-power factor, high efficiency, a wide range of economic operation states and high-power density due to the use of a built-in permanent magnet that generates a strong magnetic field [3, 6, 7]. Unfortunately, their significant disadvantage is the generation of cogging torque caused by the interaction between the magnet and stator teeth. It adversely affects the resultant starting torque and the trajectory of the driving torque, particularly in the lower speed range. To reduce the cogging torque and increase the starting torque of LSPMSMs, many scientists and development centres are looking for a new permanent magnet structure and a starting cage with a new shape. In the calculations and design of these machines with new structures and unconventional shapes, it is necessary to use software to analyse the electromagnetic field and to calculate machine parameters based on field values. There are professional FEM software packages for electromagnetic field calculations, including JMAG-Designer [8], ANSYS Maxwell [9, 10], Simcenter MAGNET [11, 12], COMSOL Multiphysics [13, 14], Opera SYMULIA [15, 16], Flux 2D [17, 18] or its three-dimensional variant Flux 3D [19, 20]. Using some of the above-mentioned FEM packages, the author has prepared and repeatedly tested independently developed FEM-based software for calculating the electromagnetic field distribution in electrical machines with permanent magnets and squirrel cage windings.

All the above-mentioned software programs and the in-house software are intended to be included in the optimization calculations and in the calculations of coupled phenomena, e.g., problems in which the equations of the electromagnetic field are solved simultaneously with the equations of the thermal field. Therefore, it is very important to minimize the calculation time. There are many papers in the literature devoted to the comparison and evaluation of professional software for field analysis of electrical machines, e.g., papers on the use of ANSYS Maxwell and COMSOL Multiphysics software. Very often, measurement verification of calculation results is presented to check the accuracy of the applied simulation models and computational software. The articles in question concern comparisons not only of the calculations of the electromagnetic field, but also of other physical fields, e.g., thermal fields, fluid flow fields, mainly in 2D [21–25]. Usually, the presented research results lead to the conclusion that there is a very high convergence of results obtained using different optical environments, e.g., ANSYS Maxwell or COMSOL Multiphysics. The disadvantages of the software used are usually not mentioned, which, apart from their price, are a large demand for operational memory and a relatively long calculation time, especially in 3D modelling. These inconveniences come mainly from the excessive universality of the computing environment used.

In view of the above, the author found it advantageous to develop his own computational software oriented to the field-circuit analysis of LSPMSMs. The article presents the results of his recent paper on the search for software to analyse LSPMSMs based on the FEM, which on the one hand, is the most reliable from the point of view of accuracy, and on the other hand, is the least time-consuming. The author compared the effectiveness of the personally-developed software with the effectiveness of professional FEM packages ANSYS Maxwell and COMSOL

Multiphysics. He compared the results of the calculations with the results of the measurements using three software programs. Experimental tests were carried out on a measuring stand built especially for this purpose.

2. Mathematical models of comparative packages

The field-circuit approach to 2D finite element modelling of the LSPMS motor has been applied in both the in-house software and professional FEM packages. The applied model consists of equations of the electromagnetic field, circuit equations of the power supply system and equations of motion. The A - V formulation has been used. This formulation leads to the following system of equations:

$$\operatorname{curl}(v \operatorname{curl} \mathbf{A}) = \mathbf{J} + \mathbf{J}_m, \quad (1)$$

$$\mathbf{J} = -\sigma(\operatorname{d} \mathbf{A} / \operatorname{d} t + \operatorname{grad} V), \quad (2)$$

$$\operatorname{div} \mathbf{J} = 0, \quad (3)$$

$$\mathbf{J}_m = \operatorname{curl} \mathbf{M}, \quad (4)$$

where: v is the reluctivity, \mathbf{J} is the current density vector, σ is the conductivity, \mathbf{J}_m is the magnetization current density vector represented in the region with permanent magnets of the magnetization vector \mathbf{M} .

The proposed model of electromagnetic phenomena considers the nonlinearity of soft magnetic materials, $\mathbf{B} = \mu(\mathbf{H})$. However, in the area with permanent magnets, the flux density \mathbf{B} is described by the magnetization vector \mathbf{M} and the field strength \mathbf{H} :

$$\mathbf{B} = \mu_0(\mathbf{H} + \mathbf{M}), \quad (5)$$

where μ_0 is the magnetic permeability of the vacuum.

In the 2D approach, the equations presented above have a simpler form. The vector magnetic potential \mathbf{A} and the current density vector \mathbf{J} have only one component, e.g. $\mathbf{A} = \mathbf{1}_z A_z$ and $\mathbf{J} = \mathbf{1}_z J_z$. In addition, from (2) and (3), a simple expression is obtained to describe $\operatorname{grad} V = \mathbf{1}_z \partial V / \partial z$ and in simply connected conducting regions $\partial V / \partial z \neq f(x, y, z)$. It follows from the above that in the area of each individual conductor $\operatorname{grad} V$ is uniform and is only a function of time, but in the area of each conductor $\operatorname{grad} V$ can be a different function of time. Therefore, it is convenient to separately consider systems composed of thin, filamentary conductors and systems with solid conductors in which eddy currents occur. In the thin conductors, it is assumed that $J_z = i / S_c$, where i is the winding/coil current, i.e., current in the conductor, and S_c is the conductor cross-sectional area. However, in the solid conductors $J_z = -\sigma(\operatorname{d} A_z / \operatorname{d} t + u / l)$, where u is the voltage across the conductor with the length l in the direction of the z -axis. Usually, the voltage u can be determined based on the assumption that the total current in solid conductors is equal to zero. With this assumption, due to symmetry, $u = 0$ is often obtained.

In general, the transient electromagnetic field in electrical machines is voltage-excited. The current i in the winding is not known in advance. Therefore, it is necessary to consider the

equations for electric circuits of the motor and the power supply system. The set of independent loop equations must be included in the model:

$$\mathbf{u} = \mathbf{R}\mathbf{i} + \frac{d}{dt}\mathbf{L}\mathbf{i} + \frac{d}{dt}\mathbf{\Phi}, \quad (6)$$

where: \mathbf{u} is the vector of supply voltages, \mathbf{i} is the vector of loop currents in windings, \mathbf{R} is the matrix of loop resistances and \mathbf{L} is the matrix of end-turn inductances, respectively, $\mathbf{\Phi}$ is the vector of fluxes linking the windings, calculated on the basis of the distribution of the magnetic vector potential.

When analysing the dynamic states of electric motors, the equations presented above are solved together with the equations of mechanical equilibrium. The classic LSPMSM motor is considered a system with one mechanical degree of freedom and motion in the direction of the angular coordinate α of the cylindrical coordinate systems r, z, α . Therefore, the mechanical equilibrium equation can be written in the following simple form:

$$J \frac{d^2\alpha}{dt^2} = T_{el} - T_L - T_f, \quad (7)$$

where: J is the moment of inertia, T_{el} is the electromagnetic torque, T_L is the load torque and T_f is the resistive torque produced in the motor bearings and fan.

Usually, the electromagnetic torque was calculated using the Maxwell stress tensor formula. For the 2D model of the considered motor, this formula has the following form:

$$T_{el} = v_0 l r_w^2 \int_0^{2\pi} (B_r B_\alpha)_{r=r_w} d\alpha, \quad (8)$$

where: l is the length of the motor core in the direction of the z coordinate, r_w is the radius of the cylindrical surface in the centre of the air gap, $B_r = B_r(\alpha)$ and $B_\alpha = B_\alpha(\alpha)$ are the functions describing the radial and tangential components of flux density for $r = r_w$, respectively.

In the in-house FE software, Formula (8) was obtained by the analysis of virtual displacement corresponding to the moving band method in the air gap [26]. Most FEM packages also use the idea of virtual displacements of the rotor in relation to the stator. However, due to the different ways of representing the change in the rotor position on the FE model, the obtained formulas differ from the formula used in the in-house software.

In the COMSOL Multiphysics and ANSYS Maxwell packages, the implementation of coupling between moving and fixed objects is carried out using a sliding technique [27, 28]. In the COMSOL Multiphysics package, the rotor and the stator are usually considered as two separate, meshed independently, geometric objects. The coupling between the rotor and the stator is done automatically. In the coupling procedure, the fulfilment of the boundary conditions is ensured. An identity pair connecting the rotating rotor frame with the fixed stator frame is created between the rotor and the stator [28]. In the ANSYS Maxwell 2D environment, a field-circuit model of the considered machine is generated using the RMxprt Design module [9]. In this module, the user defines machine parameters and then, after performing analytical calculations, can quickly generate a 2D or 3D field model. In the basic software structure, the discretisation mesh is generated automatically and can be modified manually [27].

After applying the FEM and the time-stepping method, the equations given above take the form of a system with even several hundred thousand non-linear algebraic equations. These equations can only be solved by iterative methods. In the discussed algorithm, the considered region of the LSPMSM has been divided into triangular elements. In the time-stepping method, the backward differential scheme was used. The details of the algorithm and calculation method developed by the author have been presented, among others, in [3, 29].

3. Results of simulations and measurements

In the presented comparative analysis of the considered software, the power parameters of the LSPMSM have been calculated and measured. To form the field-circuit model of the LSPMSM, the professional FEM packages ANSYS Maxwell 16.0 and COMSOL Multiphysics 5.3 were used. The in-house FE software is elaborated in the Borland-Delphi environment. The structure of the analysed motor is shown in Fig. 1. The motor has 36 drop-shaped slots in the stator and 28 bars in the rotor. Each rotor pole is formed by 3 neodymium magnets of the N38SH type arranged in the shape of a “U” inside the rotor core. The stator winding is star connected and supplied by a 3-phase balanced system of 50 Hz and 400 V line-to-line voltage. During the design process, it has been assumed that the geometry of the stator core is given in advance. The stator core shape of the mass-produced, general purpose, 3-phase, 4-pole, 3 kW output power squirrel cage

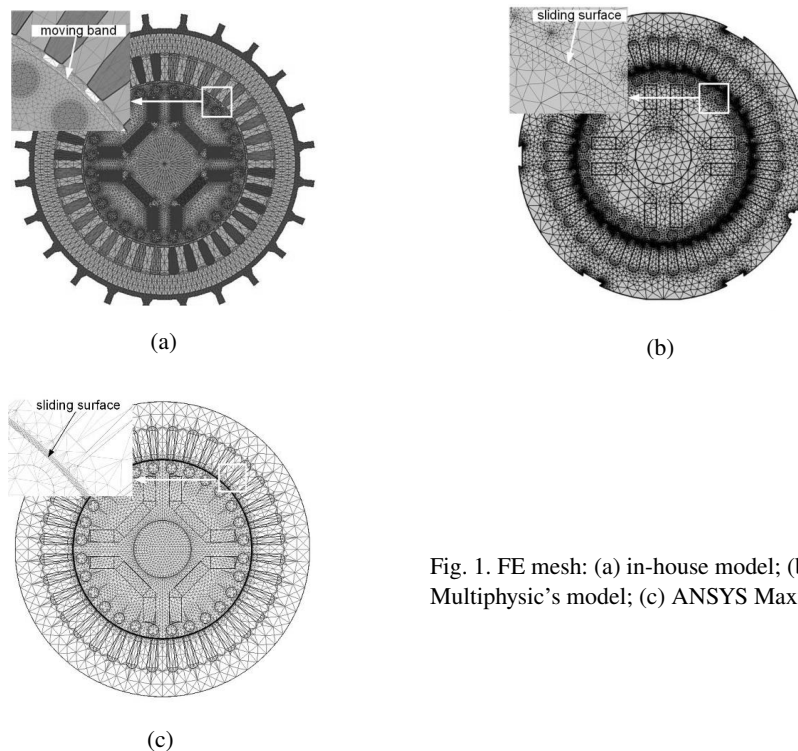


Fig. 1. FE mesh: (a) in-house model; (b) COMSOL Multiphysics model; (c) ANSYS Maxwell model

motor of the Sg100L-4B type has been used. To enable motor optimization, the rotor and stator geometries as well as supply and load system have been parameterized.

The calculations have been performed for various characteristics describing the parameters of soft and hard magnetic materials. Below, the focus is on discussing the results for the characteristics recorded in the catalogue data of the materials used in the design of the tested motor. Both the in-house software and professional software consider the nonlinearity of the magnetic material and losses in the iron into account.

The elaborated model has been utilized to investigate the influence of supply voltage on the performance and power parameters of the studied motor. The experimental verification of the calculated results was carried out. For the purposes of experimental research, a special laboratory stand with an original torque measurement system was developed – see Fig. 2. An industrial axial flow fan has been used as a load system. In order to perform tests at a variable load torque – the fan has exchangeable rotors with propeller blades set at different angles. This paper presents the results of research for two values of these angles. The load at one angle was treated as the fan A load and at the other angle as the fan B load. The load torque-speed characteristics for both fans have been shown in Fig. 3.

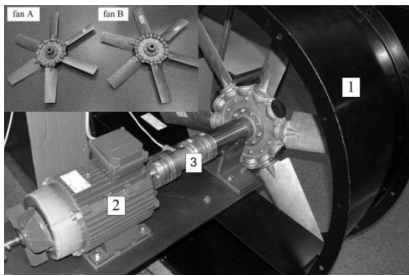


Fig. 2. Test stand: 1 – fan; 2 – LSPMSM motor; 3 – torque sensor

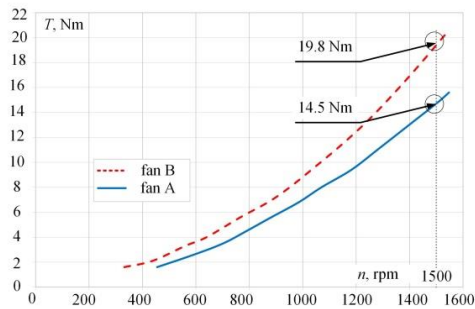


Fig. 3. Mechanical characteristics $T_L(n)$ of considered loads

The computation and measurement tests have been performed for supply voltage in the range from 250 to 525 V for two values of load torque i.e., $T_0 = 14.5$ Nm (Fig. 3, fan A) and $T_0 = 19.8$ Nm (Fig. 3, fan B). The influence of the supply voltage on the motor input power and current as well as performance factor, defined as the product of efficiency and power factor – $\cos \varphi \cdot \eta$, have been examined. In the measurements as well as simulations the supply voltage change was carried out in a steady state, after reaching the synchronous speed. During the start-up before reaching the steady state, the LSPMSM was powered by 400 V.

The calculated and measured input power and phase current have been shown in Figs. 4 and 5, respectively. However, Fig. 6 shows the measured and calculated product $\cos \varphi \cdot \eta$.

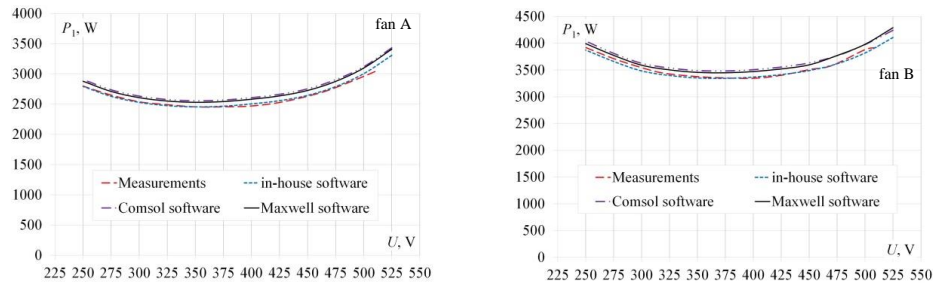


Fig. 4. Input power vs. supply voltage for two values of load torque $T_L = 14.5$ Nm (fan A) and $T_L = 19.8$ Nm (fan B)

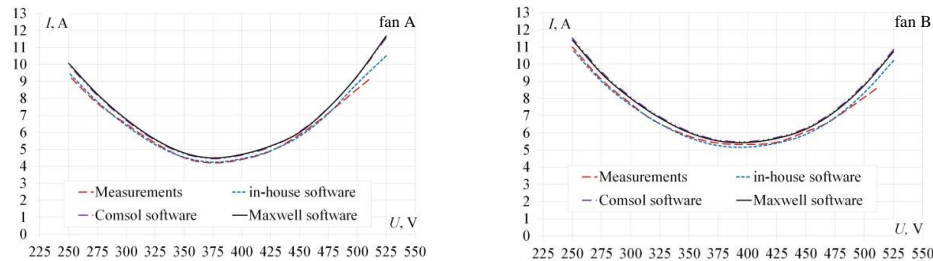


Fig. 5. Phase current vs. supply voltage for two values of load torque $T_L = 14.5$ Nm (fan A) and $T_L = 19.8$ Nm (fan B)

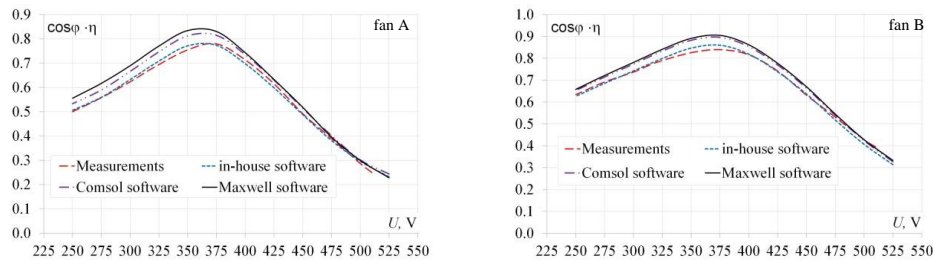


Fig. 6. Efficiency and power factor product vs. supply voltage for two values of load torque $T_L = 14.5$ Nm (fan A) and $T_L = 19.8$ Nm (fan B)

The achieved good concordance between the simulation and experiment results proves the accuracy of the developed field-circuit models, especially between the in-house software and measurements. Although the purpose of the paper is not to evaluate the designed and constructed LSPMSM, but it should be noted that the tested motor has, as intended by the designers, optimal values of parameters at a voltage of 380 V. For this value of supply voltage, the minimum of motor

current and the maximum of efficiency and power factor product can be observed. However, the performed experiments show that for such an optimal value of supply voltage, it is difficult to achieve proper synchronization of the motor, especially for a high moment of inertia of load. It has been found that setting up the rated voltage about 5% higher than optimal value improves the start-up properties of the motor, however it also causes a decrease in the power factor and leads to the inductive character of the motor.

The measured and calculated values of the power P_1 , current I , efficiency and power factor product $\cos \varphi \cdot \eta$ obtained for $T_L = 14.5$ Nm, $T_L = 19.5$ Nm at temperature $\tau = 20^\circ\text{C}$ as well as voltage $U = 400$ V are summarized in Table 1.

Table 1. Selected simulation and measurement parameters at 400 V

T_L Nm	Measured			In-house software			COMSOL Multiphysics			ANSYS Maxwell		
	P_1, W	I, A	$\cos \varphi \cdot \eta$	P_1, W	I, A	$\cos \varphi \cdot \eta$	P_1, W	I, A	$\cos \varphi \cdot \eta$	P_1, W	I, A	$\cos \varphi \cdot \eta$
14.5	2 504	4.41	0.715	2 511	4.39	0.709	2 607	4.66	0.739	2 582	4.70	0.743
19.5	3 471	5.20	0.810	3 377	5.18	0.818	3 516	5.49	0.835	3 511	5.44	0.848

The results presented in Table 1 show that the highest accuracy of the calculations in relation to the measured results was obtained using the in-house software. This was to be expected because this software was developed specifically for LSPMSM calculations.

In order to determine the relative difference between the measured and calculated results the factor $\Delta x_{\%}$ was introduced,

$$\Delta x_{\%} = \frac{|x_M - x_C|}{x_M} 100\%, \quad (9)$$

where x_M and x_C are the results obtained from the measurements and calculations (Table 1), respectively. The calculated values of the factor $\Delta x_{\%}$ for the considered operation conditions are stored in Table 2. By analysing the values given in the table it can be seen that the percentage difference between the results of the calculations and measurements does not exceed 7%.

Table 2. Summary of the factor $\Delta x_{\%}$

T_L Nm	Measured in-house software			Measured COMSOL Multiphysics			Measured ANSYS Maxwell		
	$\Delta x_{\%}$ input power	$\Delta x_{\%}$ current	$\Delta x_{\%}$ $\cos \varphi \cdot \eta$	$\Delta x_{\%}$ input power	$\Delta x_{\%}$ current	$\Delta x_{\%}$ $\cos \varphi \cdot \eta$	$\Delta x_{\%}$ input power	$\Delta x_{\%}$ current	$\Delta x_{\%}$ $\cos \varphi \cdot \eta$
14.5	0.28	0.45	0.84	4.11	5.67	3.36	3.12	6.58	3.92
19.5	2.71	0.38	0.99	1.30	5.58	3.09	1.15	4.62	4.69

Table 3 summarizes the number of FEs and computation time for three software programs used in LSPMSM calculations. The calculations have been performed on a computer with a 5-core processor of 16 GB memory. In all these calculations, the length of the time step was the same, equal to $2 \cdot 10^{-4}$ s.

Table 3. Selected simulation parameters

	In-house software	COMSOL Multiphysics	ANSYS Maxwell
Number of FEs	37 000	38 558	35 176
Time calculation	30 minutes	120 minutes	60 minutes

The total numbers of FEs in the in-house software and in the professional FEM packages are very close; however, the total computational time when using the in-house software is about 30 minutes, while ANSYS Maxwell 2016 and COMSOL Multiphysics v. 5.3 packages take between 1 and 2 hours to achieve the same small error. Thus, the calculation time for a similar number of elements is significantly shorter in the case of the in-house software application. In motors with a symmetrical magnetic circuit, we don't have to consider more than 1/4 of the entire geometry. As a result, the calculation time will be reduced. However, the relationship between the calculation times will remain the same as in Table 3, i.e., the calculation time with COMSOL Multiphysics will be 4 times longer, and with ANSYS Maxwell 2 times longer compared to the in-house software.

Whereas analysing coupled phenomena in machines with a complicated magnetic circuit, such as in the closed high-speed electric machine with excitation from the permanent magnets and liquid cooling, it is necessary to apply a 3D model. However, such a 3D model requires a spatial mesh with many times more nodes than in the 2D analysis. Solving this problem requires proportionally more computing power, and therefore the benefits of using the in-house software are even more significant than in a 2D model.

4. Conclusion

The calculations performed using the in-house software and the professional FEM packages have led to the conclusion that the in-house software has the greatest advantages. The versatility of the in-house software provides not only the ability to analyse and synthesize low- and high-power motors of any design, but also the ability to interchangeably use mathematical models of varying complexity to simulate coupled phenomena in much shorter computational time than with models developed in the professional FEM packages. The biggest advantage of the in-house software is that it can be quickly modified and special procedures can be added to determine atypical parameters that cannot be calculated in professional FEM packages, for example, procedures for determining the magnetic flux density in each elementary subarea of a permanent magnet from the magnet's demagnetization characteristics [29, 30]. This quantity allows one to evaluate and visualize the degree of partial demagnetization of permanent magnets under the influence of simultaneous changes in stator current and temperature of machine components in dynamic operating states of the LSPMSM motor.

The calculations study performed for the LSPMSM showed a high degree of agreement between the values of energy parameters calculated in COMSOL Multiphysics and ANSYS Maxwell programs. However, these results are characterized by a much greater relative difference between the results of measurements and calculations made by professional FEM packages than

the results that were calculated by the in-house program. In addition, the author observed that when deciding to choose one of the professional FEM packages analysed in the paper, many aspects should be taken into account. Using the ANSYS Maxwell package, one can quickly generate both 2D and 3D field models, which saves time in model development. Unfortunately, ANSYS Maxwell requires switching between different packages when solving multi-physics problems. If one needs access to physics and its equations in a single project and change them easily, COMSOL Multiphysics is recommended, although it requires much more operation memory.

References

- [1] de Almeida A.T., Ferreira F.J.T.E., Fong J., *Perspectives on Electric Motor Market Transformation for a Net Zero Carbon Economy*, *Energies*, vol. 16, no. 3, 1248 (2023), DOI: [10.3390/en16031248](https://doi.org/10.3390/en16031248).
- [2] Fei W., Luk P.C.K., Ma J., Shen J.X., Yang G., *A High-Performance Line-Start Permanent Magnet Synchronous Motor Amended From a Small Industrial Three-Phase Induction Motor*, *IEEE Transactions on Magnetics*, vol. 45, no. 10, pp. 4724–4727 (2009), DOI: [10.1109/TMAG.2009.2022179](https://doi.org/10.1109/TMAG.2009.2022179).
- [3] Baranski M., Szelag W., Lyskawinski W., *An analysis of a start-up process in LSPMSMs with aluminum and copper rotor bars considering the coupling of electromagnetic and thermal phenomena*, *Archives of Electrical Engineering*, vol. 68, no. 4, pp. 933–946 (2019), DOI: [10.24425/ae.2019.130693](https://doi.org/10.24425/ae.2019.130693).
- [4] Baka S., Sashidhar S., Fernandes B.G., *Design of an Energy Efficient Line-Start Two-Pole Ferrite Assisted Synchronous Reluctance Motor for Water Pumps*, *IEEE Transactions on Energy Conversion*, vol. 36, no. 2, pp. 961–970 (2021), DOI: [10.1109/TEC.2020.3029110](https://doi.org/10.1109/TEC.2020.3029110).
- [5] Kurihara K., Rahman M.A., *High-efficiency line-start interior permanent-magnet synchronous motors*, *IEEE Transactions on Industry Applications*, vol. 40, no. 3, pp. 789–796 (2004), DOI: [10.1109/TIA.2004.827476](https://doi.org/10.1109/TIA.2004.827476).
- [6] Ugale R.T., Chaudhari B.N., *Rotor Configurations for Improved Starting and Synchronous Performance of Line Start Permanent-Magnet Synchronous Motor*, *IEEE Transactions on Industrial Electronics*, vol. 64, no. 1, pp. 138–148 (2017), DOI: [10.1109/TIE.2016.2606587](https://doi.org/10.1109/TIE.2016.2606587).
- [7] Wymeersch B., De Belie F., Rasmussen C.B., Vandeveld L., *Classification Method to Define Synchronization Capability Limits of Line-Start Permanent-Magnet Motor Using Mesh-Based Magnetic Equivalent Circuit Computation Results*, *Energies*, vol. 11, no. 4 (2018), DOI: [10.3390/en11040998](https://doi.org/10.3390/en11040998).
- [8] Jun S.-B., Kim C.-H., Cha J., Lee J.H., Kim Y.-J., Jung S.-Y., *A Novel Method for Establishing an Efficiency Map of IPMSMs for EV Propulsion Based on the Finite-Element Method and a Neural Network*, *Electronics*, vol. 10, no. 9, 1049 (2021), DOI: [10.3390/electronics10091049](https://doi.org/10.3390/electronics10091049).
- [9] Aishwarya M., Brisilla R.M., *Design of Energy-Efficient Induction motor using ANSYS software*, *Results in Engineering*, vol. 16, 100616 (2022), DOI: [10.1016/j.rineng.2022.100616](https://doi.org/10.1016/j.rineng.2022.100616).
- [10] Gecer B., Tosun O., Apaydin H., Oyman Serteller N.F., *Comparative Analysis of SRM, BLDC and Induction Motor Using ANSYS/Maxwell*, 2021 International Conference on Electrical, Computer, Communications and Mechatronics Engineering (ICECCME), pp. 1–6 (2021), DOI: [10.1109/ICECCME52200.2021.9591010](https://doi.org/10.1109/ICECCME52200.2021.9591010).
- [11] Varvolik V., Prystupa D., Buticchi G., Peresada S., Galea M., Bozhko S., *Co-Simulation Analysis for Performance Prediction of Synchronous Reluctance Drives*, *Electronics*, vol. 10, no. 17, 2154 (2021), DOI: [10.3390/electronics10172154](https://doi.org/10.3390/electronics10172154).
- [12] Dobzhanskyi O., Grebenikov V., Gouws R., Gamaliia R., Hossain E., *Comparative Thermal and Demagnetization Analysis of the PM Machines with Neodymium and Ferrite Magnets*, *Energies*, vol. 15, no. 12, 4484 (2022), DOI: [10.3390/en15124484](https://doi.org/10.3390/en15124484).

- [13] Falkowski K., Kurnyta-Mazurek P., Szolc T., Henzel M., *Radial Magnetic Bearings for Rotor–Shaft Support in Electric Jet Engine*, *Energies*, vol. 15, no. 9, 3339 (2022), DOI: [10.3390/en15093339](https://doi.org/10.3390/en15093339).
- [14] Su Z., Luo L., Liu J., Li Z., Luo H., Bai H., *Research on Vibration and Noise of Induction Motor under Variable Frequency*, *Symmetry*, vol. 14, no. 3, 569 (2022), DOI: [10.3390/sym14030569](https://doi.org/10.3390/sym14030569).
- [15] Lukaniszyn M., Wrobel R., *A study on the influence of permanent magnet dimensions and stator core structures on the torque of the disc-type brushless DC motor*, *Electrical Engineering*, vol. 82, no. 3, pp. 163–171 (2000), DOI: [10.1007/s002020050007](https://doi.org/10.1007/s002020050007).
- [16] Dems M., Komezka K., Szulakowski J., Kubiak W., *Increase the Efficiency of an Induction Motor Feed from Inverter for Low Frequencies by Combining Design and Control Improvements*, *Energies*, vol. 15, no. 2, 530 (2022), DOI: [10.3390/en15020530](https://doi.org/10.3390/en15020530).
- [17] Uberti F., Frosini L., Szabó L., *A New Design Procedure for Rotor Laminations of Synchronous Reluctance Machines with Fluid Shaped Barriers*, *Electronics*, vol. 11, no. 1 (2022), DOI: [10.3390/electronics11010134](https://doi.org/10.3390/electronics11010134).
- [18] Codrean M., Simina C., Popa M., Leuca T., Giurgiu N.C., *Modelling the Process of Induction Heating in Volume of a Bar Strip Using Flux 2D Software, coupled with Minitab Experimental Design Software*, *Journal of Electrical and Electronics Engineering*, vol. 9, no. 1, pp. 5–8 (2016).
- [19] Hernández J.A.D., Carralero N.D., Vázquez E.G., *A 3-D Simulation of a Single-Sided Linear Induction Motor with Transverse and Longitudinal Magnetic Flux*, *Applied Sciences*, vol. 10, no. 19, 7004 (2020), DOI: [10.3390/app10197004](https://doi.org/10.3390/app10197004).
- [20] Islam M.S., Agoro S., Chattopadhyay R., Husain I., *Heavy Rare Earth Free High Power Density Traction Machine for Electric Vehicles*, 2021 IEEE International Electric Machines and Drives Conference (IEMDC), pp. 1–8 (2021), DOI: [10.1109/IEMDC47953.2021.9449585](https://doi.org/10.1109/IEMDC47953.2021.9449585).
- [21] Mishra R., Behera B.K., Muller M., Petru M., *Finite element modeling based thermodynamic simulation of aerogel embedded nonwoven thermal insulation material*, *International Journal of Thermal Sciences*, vol. 164, 106898 (2021), DOI: [10.1016/j.ijthermalsci.2021.106898](https://doi.org/10.1016/j.ijthermalsci.2021.106898).
- [22] Coteț F.-A., Văscan I., Szabó L., *On the Usefulness of Employing ANSYS Motor-CAD Software in Designing Permanent Magnet Synchronous Machines*, *Designs*, vol. 7, no. 1 (2023), DOI: [10.3390/designs7010007](https://doi.org/10.3390/designs7010007).
- [23] Salvi D., Boldor D., Ortego J., Aita G.M., Sabliov C.M., *Numerical Modeling of Continuous Flow Microwave Heating: A Critical Comparison of COMSOL and ANSYS*, *Journal of Microwave Power and Electromagnetic Energy*, vol. 44, no. 4, pp. 187–197 (2010), DOI: [10.1080/08327823.2010.11689787](https://doi.org/10.1080/08327823.2010.11689787).
- [24] Abdelqader M., Morelli J., Palka R., Woronowicz K., *2-D quasi-static solution of a coil in relative motion to a conducting plate*, *COMPEL – The International Journal for Computation and Mathematics in Electrical and Electronic Engineering*, vol. 36, no. 4, pp. 980–990 (2017), DOI: [10.1108/COMPEL-07-2016-0312](https://doi.org/10.1108/COMPEL-07-2016-0312).
- [25] Wang Y., Song W., Yazdani-Asrami M., Fang J., *A Fast Numerical Modeling Approach Based on Boundary Field Method for Calculating AC Losses in Superconducting Motors*, *IEEE Transactions on Applied Superconductivity*, vol. 33, no. 3, pp. 1–6 (2023), DOI: [10.1109/TASC.2023.3245039](https://doi.org/10.1109/TASC.2023.3245039).
- [26] Baranski M., Demenko A., Lyskawinski W., Szelag W., *Finite element analysis of transient electromagnetic-thermal phenomena in a squirrel cage motor*, *COMPEL – The International Journal for Computation and Mathematics in Electrical and Electronic Engineering*, vol. 30, no. 3, pp. 832–840 (2011), DOI: [10.1108/03321641111110807](https://doi.org/10.1108/03321641111110807).
- [27] <https://www.ansys.com>, accessed March 2023.

- [28] <https://www.comsol.com>, accessed March 2023.
- [29] Baranski M., Szlag W., Lyskawinski W., *Experimental and Simulation Studies of Partial Demagnetization Process of Permanent Magnets in Electric Motors*, IEEE Transactions on Energy Conversion, vol. 36, no. 4, pp. 3137–3145 (2021), DOI: [10.1109/TEC.2021.3082903](https://doi.org/10.1109/TEC.2021.3082903).
- [30] Baranski M., Szlag W., Lyskawinski W., *Analysis of the Partial Demagnetization Process of Magnets in a Line Start Permanent Magnet Synchronous Motor*, Energies, vol. 13, no. 21, pp. 5562 (2020), DOI: [10.3390/en13215562](https://doi.org/10.3390/en13215562).